Thermal emission at near-infrared wavelengths from three-dimensional copper photonic crystals

Shich-Chuan Wu, Yu-Lin Yang, Wen-Hsien Huang, and Yang-Tung Huang

Citation: Journal of Applied Physics **110**, 044909 (2011); doi: 10.1063/1.3625263
View online: http://dx.doi.org/10.1063/1.3625263
View Table of Contents: http://scitation.aip.org/content/aip/journal/jap/110/4?ver=pdfcov
Published by the AIP Publishing

Thermal emission at near-infrared wavelengths from three-dimensional copper photonic crystals

Shich-Chuan Wu,[1] Yu-Lin Yang,[2,a)] Wen-Hsien Huang,[1] and Yang-Tung Huang[2]
[1]*National Nano Device Laboratories, No. 26, Prosperity Road I, Science-based Industrial Park, Hsinchu 300, Taiwan*
[2]*Department of Electronic Engineering and Institute of Electronics, National Chiao Tung University, 1001 University Road, Hsinchu 300, Taiwan*

(Received 1 March 2011; accepted 8 July 2011; published online 25 August 2011)

A three-dimensional copper photonic crystal was fabricated with the high compatibility process, damascene copper interconnections technique. The reflectance and transmittance spectra of this structure were measured with the Fourier-transform infrared spectroscopy and simulated with the 3 D finite-difference time-domain method. From the experiment data, it is shown that this structure exhibits a large photonic bandgap from mid-infrared regime to $\lambda = 1.95$ μm. At a heating temperature of 420 °C, it is observed that thermal emission is enhanced near the bandedge $\lambda = 1.71$ μm and suppressed in the bandgap region. This is attributed to the enhancement of photonic density of states near the bandedge. © *2011 American Institute of Physics*. [doi:10.1063/1.3625263]

INTRODUCTION

In recent years, three-dimensional photonic crystals (3D PCs) have attracted great attention for their ability to control the flow of light omni-directionally for a specific range of frequencies, which is a so-called full photonic bandgap (PBG). The woodpile structure[1] is one of the proposed 3D structures that has been explored substantially. This structure has been successfully realized with dielectric or metallic materials by some state-of-the-art technologies.[2–4] However, fabricating a 3D all metallic PC with a submicron feature size in a large area is still a challenge due to their complex processing steps. One of the promising features for metallic PCs is the capability of tailoring their thermal emission spectra.[5,6] In the range of PBG, thermal emission from the 3D metallic PCs is suppressed, and narrowband emission is observed at the wavelengths near the photonic band edges. To achieve emission at shorter wavelengths, reduction of the feature sizes for the 3D lattices as well as adoption of appropriate materials to construct metallic PCs are necessary for shifting the band edges to higher frequencies. In this paper, copper was selected as the material to form the 3D lattices for its desirable optical properties at near-infrared wavelengths and high compatibility with the fabrication of damascene copper interconnections. The photonic band structures and fabrication processes for this lattice are discussed. The reflectance and transmittance spectra of the 3D copper were measured with the Fourier-transform infrared (FTIR) spectroscopy and simulated with the 3D finite-difference time-domain (FDTD) method. Through both the experimental observation and the calculation verification, the characterization of the PBG at near-infrared wavelengths is discussed. In addition, the thermal emission is investigated from the 3D copper PCs at different temperatures for revealing the property of narrowband emission at band-edge wavelengths.

EXPERIMENT

The 3D copper PCs were fabricated by the copper interconnection process. In the first step, a layer of 0.4 μm silicon oxide (SiOx) was deposited on a silicon substrate (Multiplex Cluster System, STS), patterned (FPA-3000i5 + Stepper, Canon), and etched (ILD-4100), to the top of substrate. Then, this mold was covered with 0.03 μm tantalum and 0.05 μm copper seed layers by sputter deposition (SBH-3308RDE Sputtering System, ULVAC), and filled with a copper film by copper electroplating (EP-802). The structure was then planarized to remove excess copper and tantalum by chemical mechanical polishing (CMP, model 372M, Westech). The same processes were repeated layer-by-layer as desired. At the end of the process, the SiOx mold was released from the whole structure by dilute hydrofluoric acid. The woodpile structure consists of parallel copper rods with a pitch d of 1.2 μm in each layer. The rod width w and rod height h are both 0.4 μm. The orientation of rods in one layer is perpendicular to that in the adjacent layer. The position of rods in one layer is shifted by $d/2$ with respect to that in the alternate layers. This is a so-called face-centered-tetragonal (fct) lattice. Scanning electron microscopy (SEM) was used for the morphology of 3D Cu PC observation. The PBG behaviors of the fabricated 3D woodpile copper PCs were investigated by measuring the reflectance and transmittance spectra for one- to four-layer structures with a FTIR microscope (Hyperion 2000, Bruker). The reflectance and transmittance were obtained by normalizing the measured results taken from the fabricated samples to those from a uniform gold mirror and a bare silicon wafer, respectively. To verify the measurement results, the reflectance and transmittance spectra were simulated by the 3D FDTD method with the boundary of perfectly matched layers. The computational domain was divided into $600 \times 600 \times 300$ grid points,

a)Author to whom correspondence should be addressed. Electronic mail: ylyang80@gmail.com.

corresponding to 10 grid points per rod width w in the whole space. Two time monitors placed on either side of the 3D woodpile PCs recorded the fields going through them to obtain the reflectance and transmittance. In the simulation, the geometrical parameters used were the same as the fabricated ones, and the wavelength-dependent refractive indices were also used.[7–9] The tantalum layers were ignored because their thicknesses were too thin.

For achieving thermal emission, the 3D copper PCs were thermally pumped. The copper sample mount was equipped with two cylindrical heater cartridges. The samples were sandwiched between the apertured stainless plate and the sample mount. Thermal heating of the air and convection were greatly reduced by placing the heating setup and the samples in a vacuum chamber pumped to around 10^{-5} Torr. The chamber was set on the three-axis translation stage. There is an iris diaphragm with an aperture diameter of 5 mm for blocking unwanted radiation, as shown in Fig. 1. The emitted light from the sample was collected by the parabolic mirror and fed into the FTIR spectrometer for spectral analysis. The FTIR was equipped with the CaF_2 beam splitter and the MCT detector.

RESULTS AND DISCUSSION

The SEM images of the fabricated 3D copper PCs are shown in Fig. 2. The overall sample area is 10×5 mm^2. The fabricated structure is not an ideal fct lattice. The copper rods in the fourth layers are shifted by around 0.30 μm with respect to the ideal position. Figure 2(c) is the sample with silicon dioxide mold, and Figures 2(d)–2(f) are the four-layer structures from top, tilted, and enlarged views after the SiOx released, respectively. Figure 3(a) shows the measured

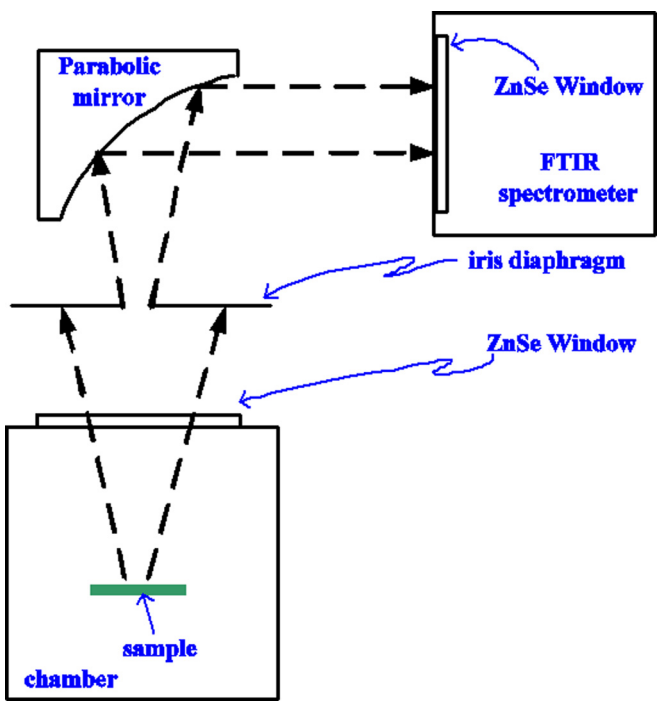

FIG. 1. (Color online) Schematic diagram of the thermal-emission measurement setup.

reflectance and transmittance spectra as functions of the number of layers. The unpolarized incident light propagates along z-direction. At wavelengths longer than 2.00 μm, the magnitude of reflectance rises when the number of layers increases. The transmittance reveals the opposite trend. For the four-layer structure, the reflectance exhibits a dip at a wavelength of 1.72 μm and some oscillations at wavelengths below 1.50 μm. Correspondingly, the transmittance shows a peak at a wavelength of 1.73 μm, which agrees with the reflectance results. Below 1.50 μm, the measured signals are too low to be detected by the detector because of the strong absorption by the silicon substrate. The measured band edge, which is defined where the reflectance is 0.5, is located at a wavelength of 1.95 μm. In particular, the reflectance dip at 1.72 μm (or the transmission peak at 1.73 μm) is close to the waveguide cutoff wavelength 1.60 μm, twice the air opening of 0.80 μm. It is attributed that the area open to the air behaviors similarly to a metallic square waveguide. Above the waveguide cutoff wavelength, only evanescent waves are observed, resulting in such a large PBG.

To gain insight into the PBG behaviors, the measured reflectances were taken with s- and p-polarized incident light, as shown in Figs. 3(b) and 3(c). Here, s and p polarization are defined as the electric fields of incident light parallel and perpendicular to the extension direction of copper rods in the outermost layer, respectively. It can be seen that the measurement results are roughly identical for s-polarization. This is because the waveguide cutoff effect plays an important role even for the case of single layer.[10] For p polarization, the forbidden bands are less sharp than those for the s polarization owing to the longer penetration length into the 3D copper PCs. This leads to stronger scattering at large angles and only the portion of the reflected light from 3D copper PCs captured by the Cassegrain objective lens. Even so, it can be observed that the band edges are shifted to the shorter wavelengths when the number of layers increases. This is the evidence for the development of the full bandgap for the 3D copper PCs. To probe the effect of tilted-angle incidence on the PBG, the measurements were performed with a grazing angle objective (Bruker) in the FTIR microscope. The incident light propagated between (001) and (110) axes of the fct lattice. Figures 3(d) and 3(e) show the measurement results for s and p polarizations, respectively. The angles of grazing incidence were between 52.2° and 84.2° off normal to the surface of the samples, as shown in the inset of Fig. 3(d). The results show that the first dips for both polarizations are shifted to longer wavelengths for the four-layer structure. This mainly stems from the shortage of the number of the stacking layers.[11]

Figure 4 shows the simulation results for the corresponding structures, which agree with the experimental data for wavelengths above 1.10 μm. This may be attributed to the fact that the 3D copper PCs exhibit stronger scattering at shorter wavelengths. The objective lens in the FTIR microscope only detects a part of the reflected signals, resulting in a discrepancy between the simulation and measurement results. In addition, the tantalum layers on the side walls of the copper rods are absorptive for wavelengths below 1.50 μm, resulting in the considerable decrease of reflectance. For

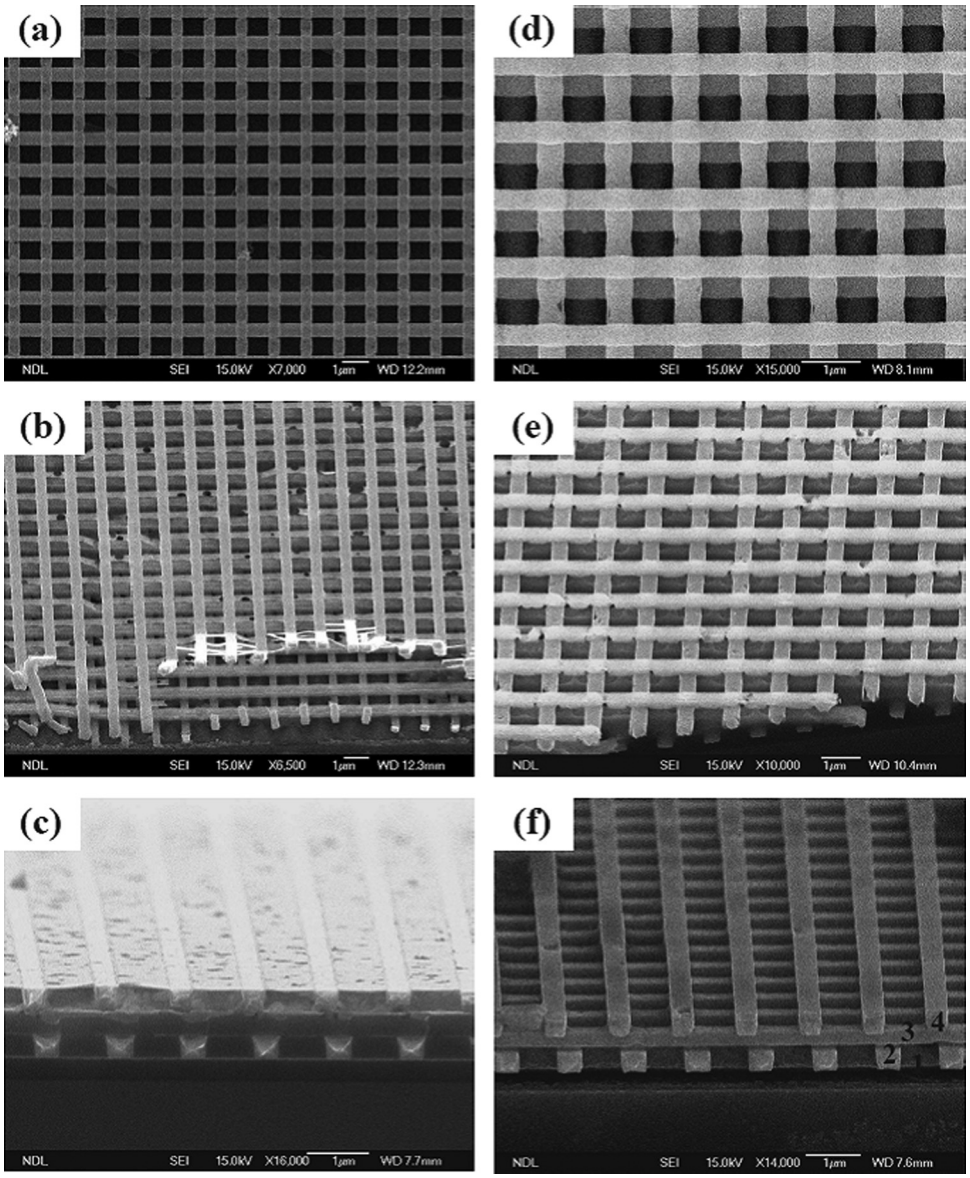

FIG. 2. SEM images of the woodpile copper PCs. The copper rod width and height are both around 0.40 μm. The rod-to-rod spacing is around 1.20 μm. (a) The two-layer structure. (b) The three-layer structure. (c) The four-layer structure with the silicon dioxide mold. (d)–(f) The four-layer structures from top, tilted, and enlarged views, respectively.

the four-layer structure, the simulation results exhibit dips at wavelengths of 1.18, 1.48, and 1.72 μm for the unpolarized incidence. The locations of dips at 1.18 and 1.72 μm show good agreement with the measurement results, but the dip at 1.48 μm has not been observed from the experimental data due to measurement deviation.

In the 3D woodpile metallic PCs, a reflectance dip corresponds to transmission and absorption peaks. The propagating mode at the lowest frequency may originate from the waveguide cutoff effect. The cutoff wavelength λ_{cutoff} is determined by the relation $\lambda_{\text{cutoff}} \approx 2\lambda_{\text{open}}\, n_f$, where λ_{open} and n_f are the length and refractive index of the open domain, respectively. For the higher-frequency propagating modes, they still approximately follow the linear scaling law with respect to n_f for a perfectly conducting structure.[12] To examine this scalability, the 3D woodpile copper PCs were measured before the release of the SiOx mold to check the position shifts of the reflectance dips. In this configuration, the filling material in the 3D copper PCs was changed from air to SiOx, as shown in Fig. 5. The positions of the three dips for the 3D copper PCs with the filling material of air are located at wavelengths $\lambda_1 = 1.72$ μm, $\lambda_2 = 1.19$ μm, and $\lambda_3 = 0.92$ μm, respectively. With the increase of the refractive index from 1.00 (air) to 1.45 (SiOx), these three reflectance dips move to longer wavelengths, $\lambda_1' = 2.60$ μm, $\lambda_2' = 1.79$ μm, and $\lambda_3' = 1.46$ μm. The relations of these dip positions are $\lambda_1'/\lambda_1 \approx 1.51$, $\lambda_2'/\lambda_2 \approx 1.50$, and $\lambda_3'/\lambda_3 \approx 1.59$. The deviation from the expected ratio 1.45 is within 10%. This may result from the change in the refractive index of SiOx after the process of chemical-mechanical polishing and from experimental errors.

A 3D metallic PC not only shows a large PBG, but also exhibits particular transmission and absorption behaviors as shown in Fig. 6(a). There exists an absorption peak at a wavelength of 1.72 μm for the four-layer copper PCs with the copper rod width of 0.40 μm, where the absorption is obtained from 1-Tr-Re. Tr and Re are the transmittance

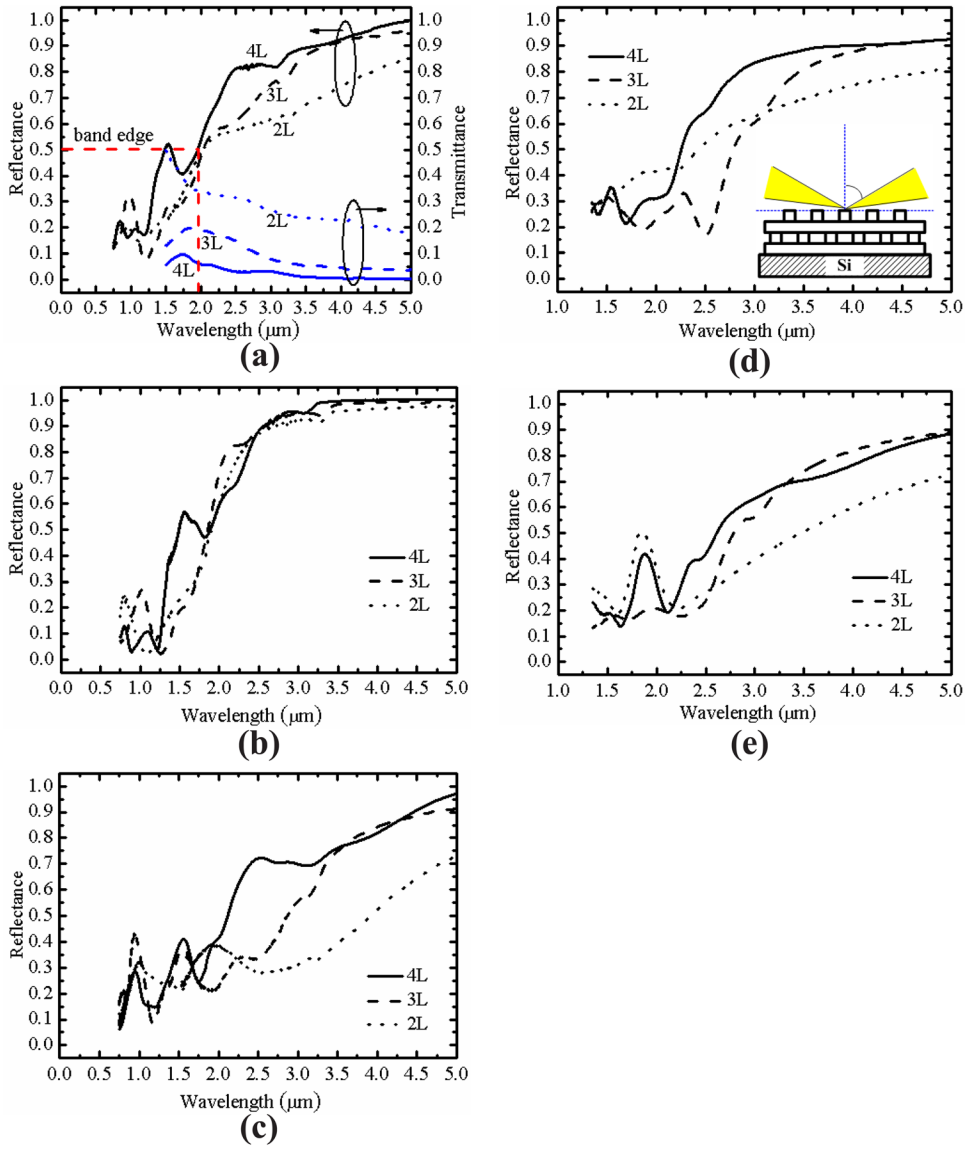

FIG. 3. (Color online) Measured reflectance spectra of the 3D copper PCs. The (a) unpolarized, (b) s-polarized, and (c) p-polarized light is normally incident along the stacking direction. The glancing-angle measurement with (d) s- and (e) p-polarized incident light for copper PCs with different numbers of layers.

and reflectance for the 3D copper PCs, respectively. For a uniform thickness copper film, the absorption is low in this wavelength range because a copper material can be approximated as a good conductor. This enhancement is attributed to the flat photonic dispersion at the band edge and the finite intrinsic absorption of copper. The flat dispersion represents a slower group velocity of light through 3D copper PCs and a longer interaction time between photon and copper, resulting in increased absorption.[13–17]

According to Kirchoff's law, the absorptance of a body equals its emissivity.[18] Within a PBG, spontaneous emission is forbidden owing to the absence of photon states that can be coupled with the atomic transition. At the band edge, the flat dispersion implies high photonic density of states (DOS), which facilitate light emission at a narrowband. Through the redistribution of the DOS, a 3D metallic PC may be useful for energy applications, such as high-efficiency light sources and thermal-photovoltaic systems.

An ideal blackbody is defined as a perfect absorber and also a perfect emitter. The hemispherical thermal radiation from the blackbody at a temperature T follows the Planck radiation law, which is given by[18]

$$I_{\mathrm{BB}}(\omega,T) = \boldsymbol{\rho}_0(\omega)u(\omega,T)\hbar\omega c/4 \tag{1}$$

where $\boldsymbol{\rho}_0(\omega)$ is the free-space DOS and has the known form of ω^2/π^2c.[3] $u(\omega,\mathrm{T})$ is the Bose-Einstein distribution function and c is the vacuum speed of light. Figure 7 shows the calculated radiation power from the blackbody at different temperatures. The majority of the radiation spectra occupies the mid-infrared range. High temperature operation is necessary to shift the emission peak to near-infrared or visible ranges. The thermal radiation from the 3D metallic PCs can be written as[17]

$$I_{\mathrm{MPC}}(\omega,T) = \boldsymbol{\alpha}_{\mathrm{MPC}}\boldsymbol{\rho}_{\mathrm{MPC}}(\omega)u(\omega,T)\hbar\omega c/4 \tag{2}$$

where α_{MPC} and ρ_{MPC} are the extraction efficiency and DOS of the metallic PCs, respectively. The redistribution of DOS and extraction efficiency of metallic PCs can be deduced from the ratio $I_{\mathrm{MPC}}(w,T)/I_{\mathrm{BB}}(w,T)$, which is also described as emissivity E. The emissivity specifies how well a real body radiates energy as compared with the blackbody.[18] In actual experiments, a spectral emissivity of a sample can be obtained from the following relation

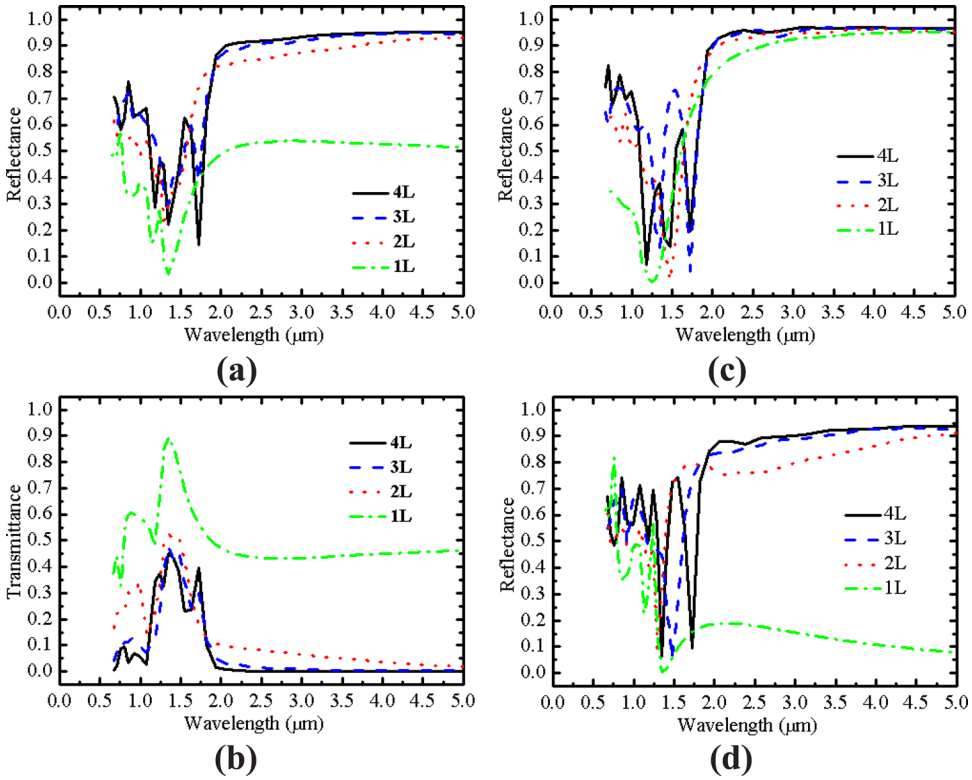

FIG. 4. (Color online) Simulated reflectance and transmittance spectra of the 3D copper PCs of the same dimensions as the fabricated one. (a), (b) The normal incident light is unpolarized. The normal incident light is (c) s-polarized and (d) p-polarized.

$$E_{\text{sample}}(\lambda,T) = S_{sample}(\lambda,T) \times E_{reference} / S_{reference}(\lambda,T) \quad (3)$$

where $S_{sample}(\lambda,\text{T})$ and $S_{reference}(\lambda,\text{T})$ are the measured emission spectra from a sample and the reference material at a temperature T, respectively. In our case, blackbody paint was used as a reference material with the temperature-independent emissivity $E_{\text{reference}}$ of 0.94. The measured emissivity can be expressed as $E_{sample} = E_{copper\ PCs} + E_{Si} \times T_{pc}$,[19] where E_{Si} and T_{pc} are the emissivity of silicon substrate and transmittance of the 3D copper PCs, respectively. The measured emissivity of the silicon substrate is around 0.77, which is wavelength independent at our measurement temperatures. We eliminated the measured emissivity contributed from the silicon substrate to obtain the emissivity of 3D copper PCs

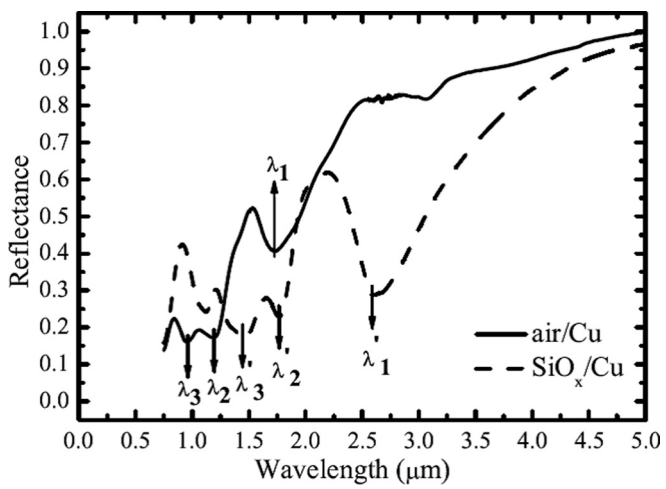

FIG. 5. Measured reflectance spectra of 3D copper PCs with the filling materials of air and SiOx.

$E_{\text{copper PCs}}$, as shown in Fig. 6(b). The emissivity spectra for the four-layer copper PCs show similar trends at different temperatures and agree with the absorptance spectrum. The magnitude of the emissivity in the entire measurement range is higher than that of absorptance. This may be attributed to the fact that the outermost layer in the 3D PCs experiences slight PBG effect and increases the absorption at higher temperatures.

The dips at wavelengths around 4.25 μm are caused by absorption from the carbon dioxide (CO_2) in the environment. The emission peaks at wavelengths around 3.10 μm, also observed in the absorptance spectrum, are mainly due to the absorption for p-polarized incidence. The dominant peaks near the band edge are located at wavelengths of 1.71, 1.63, and 1.60 μm at heating temperatures of 420, 450, and 480 °C, respectively. Compared with the absorption peak at 1.72 μm, the deviations are all within 7%. The temperature dependence for these peaks may be attributed to the thermal gradients across the samples and uncertainty in the probe of the temperatures. However, the experimental data do show the enhancement of the thermal emission near the band edge. For the purpose of comparison, the emissivity of copper material is below 0.1 at high temperatures.[20] For the blackbody, temperature as high as 1504 °C is required to shift the radiation peak to 1.62 μm. Therefore, the 3D copper PCs can be applied as high-efficiency light sources at near-infrared wavelengths.

CONCLUSION

3D copper PCs with fct lattice have been fabricated using the high compatibility processes of damascene copper

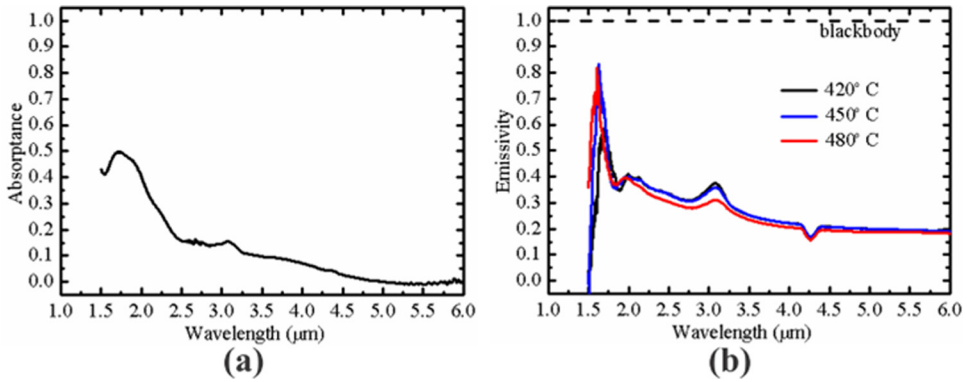

FIG. 6. (Color online) (a) Absorptance spectra for the four-layer copper PCs. (b) Measured emissivity for the same structure at different temperatures.

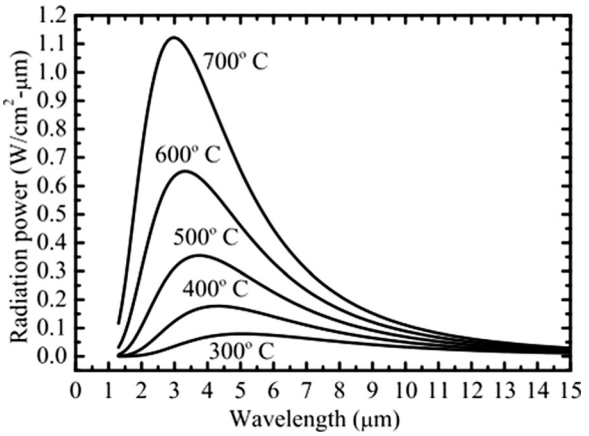

FIG. 7. Radiation curves of the blackbody at different temperatures.

interconnections. The structure has parameters of $w/h/d = 0.40/0.40/1.20$ μm and its characterization is discussed at near-infrared wavelengths. The optical properties of PBGs for the copper PCs have been investigated by experimental observation and simulation verification. In the stacking direction, it was experimentally observed that the photonic band edge is located at wavelengths of 1.95 μm for unpolarized normal incidence. It is also shown that the propagating modes in our structures are able to be scaled by the refractive index of the mold in the 3D PCs. Furthermore, the enhanced thermal emission near the band edge wavelength of 1.71 μm has been experimentally observed at a heating temperature of 420 °C. The deviation of the emission peak is within 7% for temperature rising to 480 °C.

ACKNOWLEDGMENTS

The authors would like to thank Professor Shawn-Yu Lin of Rensselaer Polytechnic Institute for valuable discussion about the characterization of thermal emission from 3D PCs. This work was supported in part by National Science Council of Taiwan (NSCT) under Contract No. 98-2221-E-492-020 and by National Nano Device Laboratories for the project of nanometer-scaled 3D metal PCs.

[1]K. M. Ho, C. T. Chan, C. M. Soukoulis, R. Biswas, and M. Sigalas, Solid State Commun. **89**, 413 (1994).
[2]S. Y. Lin, D.-X. Ye, T.-M. Lu, J. Bur, Y. S. Kim, and K. M. Ho, J. Appl. Phys. **99**, 083104 (2006).
[3]J.-H. Lee, C.-H. Kim, Y.-S. Kim, K.-M. Ho, and C. H. Oh, Appl. Phys. Lett. **88**, 181112 (2006).
[4]V. Mizeikis, S. Juodkazis, R. Tarozaite, J. Juodkazyte, K. Juodkazis, and H. Misawa, Opt. Express **15**, 8454 (2007).
[5]S. Y. Lin, J. Moreno, and J. G. Fleming, Appl. Phys. Lett. **83**, 380 (2003).
[6]J.-H. Lee, Y.-S. Kim, K. Constant, and K.-M. Ho, Adv. Mater. (Weinheim, Ger.) **19**, 791 (2007).
[7]E. D. Palik, *Handbook of Optical Constants of Solids* (Academic Press, London, 1985).
[8]M. A. Ordal, L. L. Long, R. J. Bell, S. E. Bell, R. R. Bell, R. W. Alexander, Jr., and C. A. Ward, Appl. Opt. **22**, 1099 (1983).
[9]I. El-Kady, M. M. Sigalas, R. Biswas, K. M. Ho, and C. M. Soukoulis, Phys. Rev. B **62**, 15299 (2000).
[10]Z.-Y. Li, I. El-Kady, K.-M. Ho, S. Y. Lin, and J. G. Fleming, J. Appl. Phys. **93**, 38 (2003).
[11]J. G. Fleming, S. Y. Lin, I. El-kady, R. Biswas, and K. M. Ho, Nature **417**, 52 (2002).
[12]H.-Y. Sang, Z.-Y. Li, and B.-Y. Gu, Phys. Rev. B **70**, 066611 (2004).
[13]Y.-L. Yang, F.-J. Hou, S.-C. Wu, W.-H. Huang, M.-C. Lai, and Y.-T. Huang, Appl. Phys. Lett. **94**, 041122 (2009).
[14]A. Tal, Y.-S. Chen, H. E. Williams, R. C. Rumpf, and S. M. Kuebler, Opt. Express **15**, 18283 (2007).
[15]S.-Y. Lin, J. G. Fleming, and I. El-Kady, Appl. Phys. Lett. **83**, 593, 2003.
[16]S. Y. Lin, J. G. Fleming, Z. Y. Li, I. El-Kady, R. Biswas, and K. M. Ho, J. Opt. Soc. Am. B **20**, 1538 (2003).
[17]S.-Y. Lin, J. G. Fleming, and I. El-Kady, Opt. Lett. **28**(20), 1909 (2003).
[18]K. Siegel and J. R. Howell, *Thermal Radiation Heat Transfer* (Hemisphere, Bristol, PA, 1992).
[19]T. S. Luk, T. Mclellan, G. Subramania, J. C. Verley, and I. El-Kady, Photonics Nanostruct. Fundam. Appl. **8**, 81 (2008).
[20]K. G. Ramanathan and S. H. Yen, J. Opt. Soc. Am. **67**(1), 32 (1977).